Experimental Validation of an Extended Kalman Filter for Retained Fluid Volume Estimation in Peritoneal Perfusion Applications

Yejin Moon[1], Behzad KadkhodaeiElyaderani[1], Joshua Leibowitz[2], Morcos A. Awad[2], Warren Naselsky[2], Stephen Stachnik[2], Shelby Stewart[2], Joseph S. Friedberg[3], Jin-Oh Hahn[1], and Hosam K. Fathy[1,*]

***Abstract*— This paper is motivated by peritoneal perfusion: the circulation of fluid through the abdomen of a patient or laboratory animal. Peritoneal perfusion applications include dialysis, drug delivery, and potentially providing supplemental oxygen to patients with respiratory failure. If an excessive fluid volume is retained in the abdomen during perfusion, medical complications, such as intra-abdominal hypertension and abdominal compartment syndrome, may arise. Previous work by the authors presents a state-space model of the abdominal cavity pressure dynamics causing such complications and proposes an extended Kalman filter (EKF) that uses these dynamics for retained volume estimation. In this paper, the authors aim to validate the EKF's performance using data from clinical experiments on two Yorkshire swine, which are different from the animal originally used for system identification and EKF design. In both experiments, the EKF runs online as perfusion takes place. The EKF-based volume estimate is then compared to a weight sensor-based estimate of the total fluid supplied to the animal plus the tubing connected to the animal. The two volume estimates correlate linearly, with an encouraging coefficient of determination of 91.6% for both animal experiments.**

I. INTRODUCTION

Peritoneal perfusion is the process of circulating a fluid through the abdominal (peritoneal) cavity of a patient or laboratory animal. It typically involves surgically inserting one or more catheters into the abdomen, then using these catheters for fluid circulation or "perfusion". Peritoneal perfusion is particularly attractive because the lining of the abdomen, known as the *peritoneum*, has a large surface area and a high degree of vascularization, which are two factors that facilitate rapid diffusion-based transport.

One existing clinical application of peritoneal perfusion is peritoneal dialysis. In this application, an aqueous solution is perfused through the abdomen, facilitating the diffusion-based removal of waste products. The abdomen essentially becomes a "third kidney". Oxygen delivery is a second potential application of peritoneal perfusion. The intent of this application is to use the abdomen as a "third lung" that can potentially provide supplemental oxygen to patients suffering from respiratory failures such as COVID-19. In this case, the perfused fluid is an oxygen carrier, such as an oxygenated perfluorocarbon or a foam containing oxygen microbubbles. Perfluorocarbons (PFCs) are clear, dense liquids that can dissolve exceptionally high amounts of oxygen and carbon dioxide. These solubility properties make PFCs particularly interesting as potential "third lung" oxygen carriers.

Previous work by the authors examines the effectiveness of peritoneal perfusion of an oxygenated PFC as a "third lung" treatment for respiratory failure [1]. In more recent work, we develop an instrumented setup intended for additional perfusion experiments [2] and utilize this setup for examining the effectiveness of PFC perfusion as a pathway for carbon dioxide removal [3].

Regardless of the application of interest, it is critical to perform peritoneal perfusion safely. The amount of fluid retained within the abdomen during perfusion is known as intra-abdominal volume (IAV), and can directly impact intra-abdominal pressure (IAP) [4]. Values of IAP above $12\ mmHg$ can cause an unhealthy condition known as intra-abdominal hypertension (IAH) [5]. Moreover, if IAH persists for a significant amount of time or if IAP exceeds $20\ mmHg$, patients may develop abdominal compartment syndrome (ACS). In turn, this can cause organ failure [5], [6]. Some patients in the intensive care unit develop IAH during their hospital stays, even without peritoneal perfusion [7], [8]. This makes it important to manage and control perfusion in a way that minimizes the risk of IAH and ACS.

There is extensive literature on modeling the elasticity and pressure dynamics of the abdominal cavity. This literature builds on experimental studies performed using different animal models and diverse populations [9], [10], [11] under various medical applications, such as abdominal paracentesis, laparoscopic pneumoperitoneum, and peritoneal dialysis [12], [13]. Much of the early literature assumes cavity pressure (IAP) to be related to retained volume (IAV) through a linear or affine elastic relationship [9], [10], [14], [15]. More recent studies claim that such a relationship is accurate only for IAP $< 15\ mmHg$, with significant stiffening at higher retained volumes [16], [17].

The above literature shows that cavity pressure can change significantly based on different body positioning angles [9], [10], [18], different abdominal regions [19], and a patient's condition such as pregnancy, obesity, and age [20], [21], [22], [23]. Furthermore, abdominal cavity compliance can change due to prior surgical interventions, chronic medical conditions, and varying sizes of the abdominal cavity in different individuals [24], [25]. Our previous work also highlights the fact that cavity pressure dynamics depend not only on cavity elasticity, but also on the drainage characteristics of the cavity outflow cannulas [26]. Finally, the effectiveness of diffusion-based transport depends on IAV [27]. Collectively,

Author affiliations: [1] University of Maryland School of Engineering, College Park,MD; [2] University of Maryland School of Medicine, Baltimore, MD; [3] Temple University, Philadelphia, PA; * Corresponding author (hfathy@umd.edu).

these factors make it important to monitor and estimate both IAP and IAV (i.e., retained fluid volume) online during peritoneal perfusion applications.

Previous work by the authors develops state-space models of abdominal cavity pressure dynamics, parameterizes these models using experimental studies on Yorkshire swine, and uses them to develop an extended Kalman filter (EKF) for retained fluid volume estimation [26], [28]. The EKF assumes that the following three quantities are measured in real time: the perfusion inflow rate, IAP, and any negative (i.e., suction) pressure applied externally to the perfusion outflow port. The prediction component of the EKF estimates the fluid outflow rate using a simple pressure difference-based fluid drainage model, and integrates the difference between the measured inflow rate and this outflow rate to estimate IAV. The correction component of the EKF uses IAP measurements, together with a cavity elasticity model, to furnish a closed-loop IAV estimate. In this context, the use of feedback estimation is valuable because it avoids the potential estimation drift associated with the open-loop integration of the difference between perfusion inflow and outflow rates. Furthermore, this approach is potentially more reliable than simpler strategies such as using the weight of the subject, considering that external factors, such as the accidental placement of additional weights on the operating table, can potentially jeopardize the accuracy of these approaches.

The goal of this paper is to validate the above retained fluid volume estimator using clinical experiments on Yorkshire swine. We perform this validation using experiments on two laboratory animals that are different from the animal used for EKF algorithm development. All three animals were used for oxygenated PFC perfusion experiments and were treated humanely in accordance with an approved Institutional Animal Care And Use Committee (IACUC) protocol at the University of Maryland School of Medicine. The EKF ran online, in real time, during the two validation experiments. Moreover, the perfused volume estimate of the algorithm is compared to an estimate of the total volume of fluid provided to the animal plus the perfusion cannulas. The latter estimate is calculated based on the weight of the PFC remaining in the experimental setup during the experiments, which was not available in the previous experiments. A strong linear correlation was found between these two different volume estimates for both animals.

The remainder of the paper is organized as follows. Section II describes the setup used in the animal experiments. Section III introduces the governing equations of the perfused volume estimator. Section IV analyzes the estimator's performance during the validation experiments, as well as the insights gathered from the results. Lastly, Section V summarizes the paper's conclusions.

II. EXPERIMENTAL SETUP

Fig. 1 provides a high-level schematic of the perfusion setup used in the two animal experiments, building on earlier setup design and instrumentation work in a companion article [2]. A peristaltic pump (pump A) draws the oxygenated

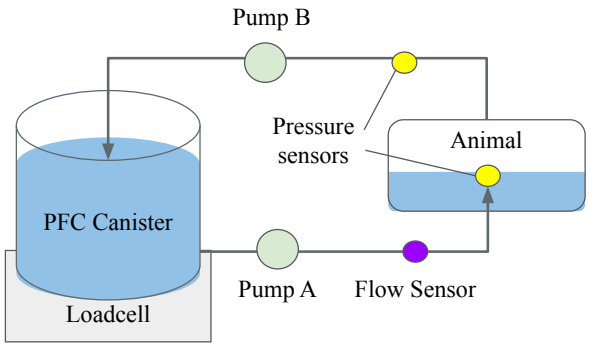

Fig. 1. Perfusion Setup

PFC from the PFC canister and supplies it to the animal. A flow sensor is incorporated into the inflow line to measure the volumetric PFC flowrate. Another peristaltic pump (pump B) is placed on the outflow line to actively drain the PFC out from the animal. A pressure sensor is mounted on the outflow line to measure the suction pressure (ambient pressure). A scale (or load cell) under the PFC canister measures the amount of PFC left in the canister. A catheter is placed inside the animal and connected to a pressure sensor in order to measure the animal's IAP.

In both validation experiments, perfusion was performed on adult male Yorkshire swine with masses of $55 - 60\ kg$, anesthetized for the entire duration of the experiments. A cis-\trans- perfluorodecalin mix is supplied to and drained from the test animals through 36 French (i.e., $12\ mm$ diameter) venous cannulas terminating in foam-covered custom diffusers. At the beginning of the experiment, the amount of PFC required to fill these cannulas was measured by observing the change in the weight of PFC in the setup's canister. The mass of the PFC needed to completely fill the inflow and outflow catheters was approximately $3.06\ kg$, which is equivalent to $1.6\ L$ of PFC.

During perfusion experiments, the perfused volume estimator received the following measurement signals: PFC inflow rate provided by Pump A, the suction pressure supplied by Pump B, and the IAP measurements from the abdominal catheter which is used to estimate IAV in real time. Two fluid volume estimates were compared using two separate sets of sensors: the estimated IAV from the perfused volume estimator (EKF IAV) and the benchmark estimate of fluid volume from the weight sensor under the PFC canister (benchmark IAV).

III. DESIGN OF EKF-BASED PERFUSED VOLUME ESTIMATOR

In this section, the equations of the EKF algorithm from the previous article are summarized [28]. The perfused volume estimator uses a simple non-linear cavity pressure dynamics model as its plant model. This model can potentially be parameterized to represent different animals' and humans' IAP-IAV relationships. This model, together with the time-varying feedback gain $K(t)$, constitutes the extended Kalman filter below:

$$\begin{aligned} \frac{d\hat{V}(t)}{dt} &= Q_{in}(t) - C_o\delta\hat{P}(t) + K(t)[P(t) - \hat{P}(t)] \\ \delta\hat{P}(t) &= \hat{P}(t) - P_\infty \\ \hat{P}(t) &= \beta_1\hat{V}(t) + \beta_2\hat{V}^2(t) + \beta_3\hat{V}^3(t) \end{aligned} \quad (1)$$

In the above equation, $\hat{V}(t)$ and $\hat{P}(t)$ represent the estimates of IAV and IAP by the observer, in Liters and $mmHg$, respectively. The underlying first-order state-space model assumes IAV and IAP to have a cubic relationship characterized by the three constants β_1, β_2, and β_3. By adjusting these coefficients, we can adjust the model to account for varying IAP-IAV characteristics. The rate of change of the IAV estimate, $d\hat{V}(t)/dt$, is the difference between the PFC inflow rate measured by the flowrate sensor, Q_{in}, and the PFC outflow rate, which is characterized as a product of a discharge constant, C_o, and the drainage pressure difference, δP. The drainage pressure difference was obtained by taking a difference between $\hat{P}(t)$ and the sensor measurement of the ambient pressure, P_∞. In order to calculate the time-varying Kalman gain, $K(t)$, the Algebraic Ricatti Equation (ARE) was applied to a linearization of the cavity pressure dynamics model around $\hat{V}(t)$. In solving the ARE, the process noise variance was set to $\mathcal{W} = 2.5 \times 10^{-3}$ $L^2 s^{-2}$, and the sensor noise variance was set to $\mathcal{V} = 0.25$ $mmHg^2$. The resulting gain was multiplied by the error between the sensor measurement of IAP, $P(t)$, and the estimated IAP, $\hat{P}(t)$, to enable the feedback-based correction of the IAV estimate over time. In this state-space estimator model, the PFC inflow rate and the suction pressure are the input variables, IAP is the output variable, and IAV is the state variable. The proposed EKF assumes the values of the model parameters C_o and $\beta_{1,2,3}$ to be known *a priori*. The work in this paper obtains these parameter values from a previous animal experiment [26], then validates the EKF using two other animal experiments. The table below summarizes the variables and parameters in Eq. (1) with their dimensions and optimally parameterized values [26], if applicable.

Symbol	Definition	Value	Units
$\hat{P}(t)$	Estimated IAP	–	$mmHg$
$P(t)$	Measured IAP	–	$mmHg$
$\hat{V}(t)$	Estimated IAV	–	L
Q_{in}	Measured PFC inflow rate	–	L/min
C_o	Discharge constant	0.0733	$L/min/mmHg$
δP	Drainage pressure difference	–	$mmHg$
P_∞	Measured ambient pressure	–	$mmHg$
β_1	P-V relationship coefficients	11.897	$mmHg/L$
β_2	P-V relationship coefficients	-5.526	$mmHg/L^2$
β_3	P-V relationship coefficients	1.193	$mmHg/L^3$
$K(t)$	Kalman gain	–	–

TABLE I
LIST OF VARIABLES AND PARAMETERS

The above algorithm, assuming the plant model to be accurate, predicts the rate of change of IAV over time using its current IAP estimate plus the two input signals: the PFC inflow rate and the ambient suction pressure. Then, it corrects its estimate by feeding back the error between the measured and the estimated IAP with the time-varying Kalman gain. Over time, the estimated IAV becomes more and more accurate using the feedback, potentially providing some degree of robustness to modeling errors, including errors in modeling the cavity drainage rate (e.g., errors in estimating C_o, etc.). The details of the calculation and the development of this algorithm can be found in the previous article [28].

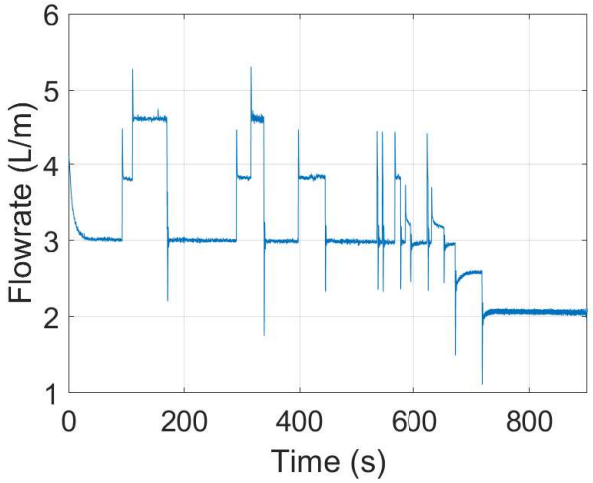

Fig. 2. PFC inflow rate (Experiment 1)

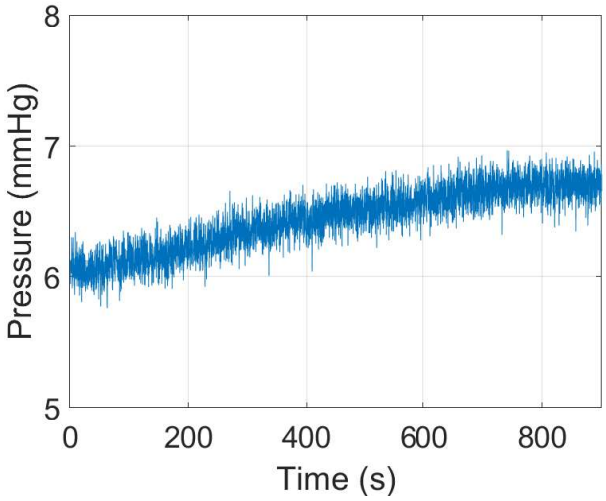

Fig. 3. Ambient pressure (Experiment 1)

IV. PERFORMANCE OF THE PERFUSED VOLUME ESTIMATOR

In this section, the collected data from the two animal experiments are analyzed to determine the performance of the perfused volume estimator in predicting IAP and IAV online using PFC inflow rate and suction pressure.

Fig. 2 and Fig. 3, respectively, show the PFC inflow rate and the ambient pressure from the first experiment over a 900

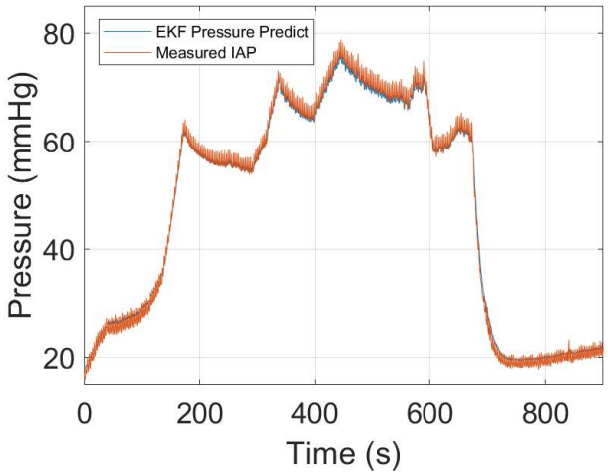

Fig. 4. Measured and the estimated IAP (Experiment 1)

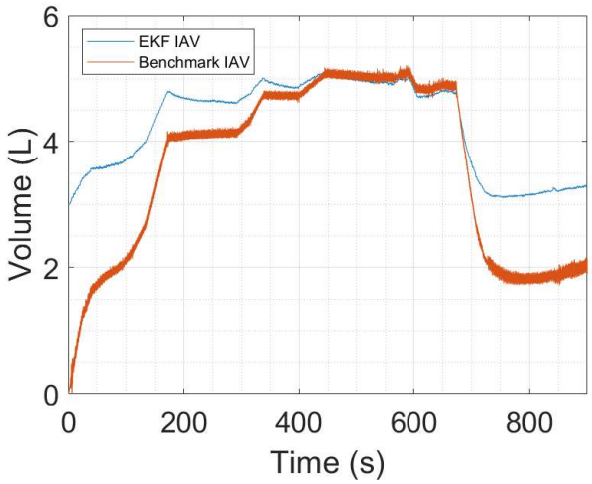

Fig. 5. IAV estimates (Experiment 1)

seconds time horizon. During the first 600 seconds, perfusion flowrate fluctuates between 3 L/min and 4.5 L/min. Then, during the rest of the time horizon, the flowrate gradually decreases to 2 L/min. A relatively consistent ambient pressure with a value between 6 $mmHg$ and 7 $mmHg$ is applied to the animal throughout this time window.

Fig. 4 compares the measured and the estimated IAP. The estimated IAP closely follows the measured IAP signal, showing that the perfused volume estimator can track the measured IAP signal well. The combination of sizable inflow rates and low ambient pressures causes IAP to increase rapidly at the beginning of the experiment. Then, as the inflow rate decreases, the IAP decreases at the 750- second mark and stays small during the rest of the experiment.

Fig. 5 compares the two different volume estimates obtained using the PFC canister's weight sensor data and the perfused volume estimator. Although there are errors between these two estimates, they have similar trends of rapid increase at the beginning of the time horizon and a decrease towards the end of the experiment.

To compare the EKF IAV and benchmark IAV, we used linear regression to fit a straight line to these two signals, as shown in Fig. 6. This fit can be expressed as $y = 0.4011x + 2.264$, where y represents the estimated IAV from the perfused volume estimator using the EKF algorithm, and x denotes the benchmark IAV estimate from the PFC canister weight change data. This regression equation implies that when the benchmark signal experiences a 1 L increase, the perfused volume estimator predicts the IAV to change by 0.4011 L.

Multiple potential explanations may exist for the differences between these two fluid volume estimates. First, the two estimates pertain to different physical quantities, with the EKF algorithm attempting to only estimate the IAV in the abdominal cavity while the benchmark IAV estimate accounts for the significant additional fluid supplied to the setup's tubing. Second, differences between the two estimates may also arise from modeling errors. One interesting observation, for instance, is that the IAV estimate by the EKF converges more closely to the benchmark signal when IAV is close to 5 L. This raises the possibility that the plant model in the EKF algorithm may not be an accurate representation of the cavity pressure dynamics for lower IAP/IAV ranges. Third, it is possible that the effective cavity stiffness was significantly different for the laboratory animals used for algorithm validation, compared to the algorithm used for EKF model parameterization. Regardless of the precise causes for the above differences in retained fluid volume estimates, it is quite encouraging that the coefficient of determination (or "R squared") value associated with the above straight-line correlation is 0.916. This means that 91.6% of the variations in the two IAV estimates can be explained via this linear correlation. This is a promising result, suggesting that it may be possible to calibrate the EKF algorithm's output signal to obtain an accurate IAV estimate.

Fig. 7 and Fig. 8 show, respectively, the PFC inflow rate and the mass of the PFC retained inside the perfusion setup's canister during the second validation experiment, over a

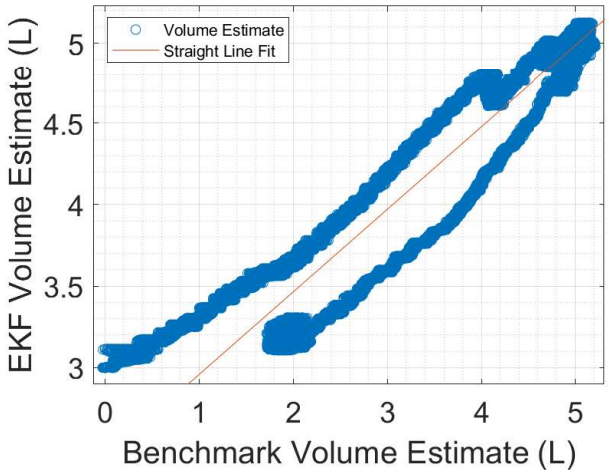

Fig. 6. Linear Regression (Experiment 1)

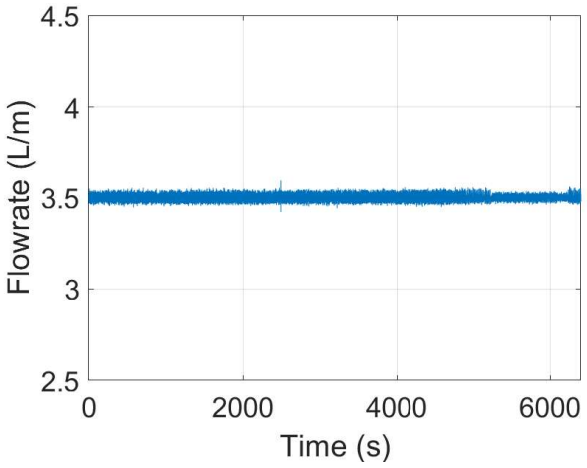

Fig. 7. PFC inflow rate (Experiment 2)

6400s time horizon. The latter quantity is measured using the canister weight sensor. Moreover, a closed-loop PI controller manipulates the flowrate command to the peristaltic suction pump (or "pump B") to track a desired staircase pattern of this latter quantity versus time, as shown in the figure.

Fig. 9 compares the measured and the estimated IAP during the second validation experiment. As a result of the above commanded staircase pattern of fluid mass versus time, IAP experiences multiple distinct upwards jumps versus time. Again, the IAP estimate by the perfused volume estimator very closely follows the measured IAP signal, validating the ability of the EKF algorithm to track this measured output signal. Fig. 10 plots the IAV estimates from the EKF and the benchmark method versus time. Once again, a staircase pattern is observed, with multiple distinct jumps in retained fluid volume within the animal's abdomen versus time. Similar to the results from the first validation experiment, the two IAV signals experience are much closer to each other at higher IAV/IAP values. This further emphasizes the possibility of an error in modeling cavity pressure dynamics,

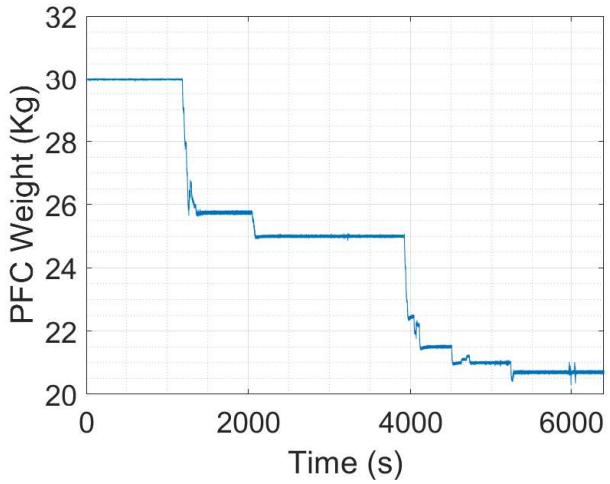

Fig. 8. Canister fluid mass history (Experiment 2)

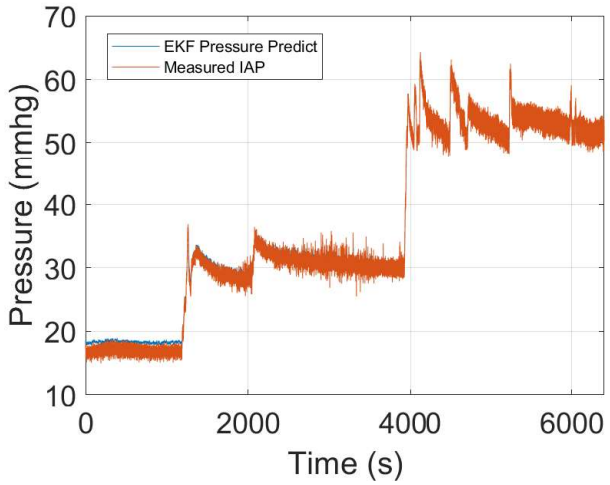

Fig. 9. Measured and the estimated IAP (Experiment 2)

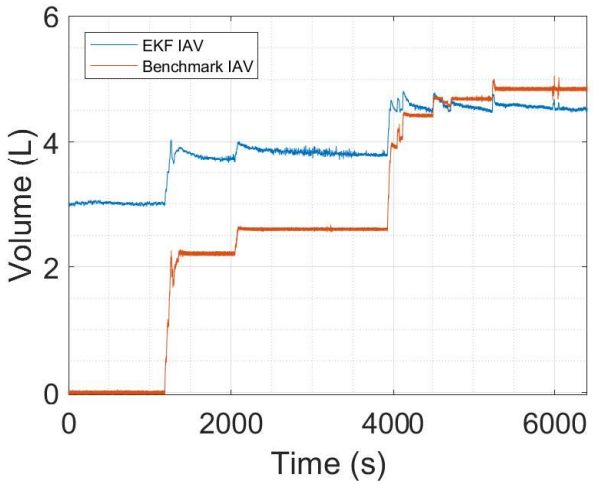

Fig. 10. IAV estimates (Experiment 2)

particularly at lower IAP/IAV values.

Linear least squares regression was used to fit a mapping between the benchmark and EKF-based estimates of IAV. The resulting straight line fit between these signals is shown in Fig. 11. The straight line fit can be expressed as $y = 0.4505x + 2.7097$, with y denoting the IAV prediction by the EKF algorithm and x denoting the benchmark IAV prediction. This relationship implies that when the PFC in the setup experiences a change in 1 L, the EKF algorithm will predict 0.4505 L change in its IAV estimate. Furthermore, there was a perfused volume-independent inconsistency of 2.7097 L between these two signals during the second experiment. Again, possible explanations for these discrepancies include modeling errors as well as potential differences in abdominal cavity compliance between the validation experiments and the previous animal experiment used for EKF algorithm parameterization. Nonetheless, the R-squared value for the straight line fit is 0.916, meaning that 91.6% of these data points can be explained by using this linear correlation. Once

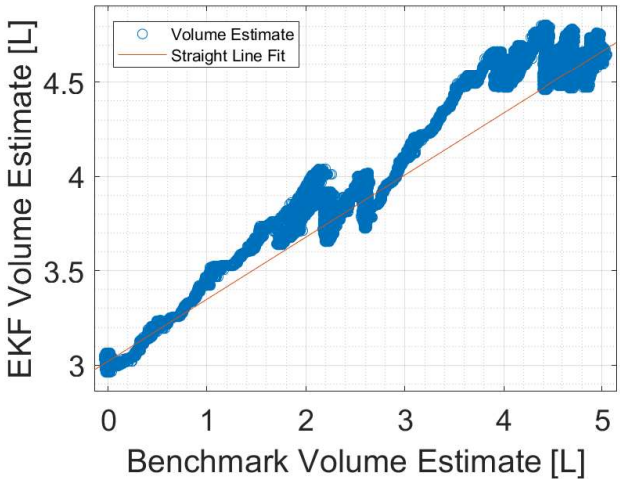

Fig. 11. Linear Regression (Experiment 2)

again, this is a very positive and encouraging result, suggesting that the perfused volume estimator, perhaps coupled with regression-based tuning, can serve as a foundation for accurate IAV estimation.

V. CONCLUSIONS

This paper demonstrates and analyzes the performance of the perfused volume estimator in predicting IAP and IAV during the two animal experiments using an Extended Kalman Filter. A good fit was obtained between the measured and the estimated IAP in both experiments. Although the benchmark IAV estimate and the EKF IAV estimate do not converge at a lower range of IAP/IAV, a strong R-squared value of 0.916 was obtained between these two signals. Altogether, these results show that the perfused volume estimator somewhat succeeds in robustly predicting IAV, given two different cavity pressure dynamics and the two slightly different sizes of the test animals. At least two contributions were made to the literature: *i*) experimentally validating a novel retained volume estimation algorithm using two different animals, and; *ii*) use of a weight sensor to measure the weight of the PFC in the setup, a measurement that was unavailable in the previous research and served as a benchmark for retained fluid volume estimation by the Extended Kalman Filter algorithm. One important topic for future research is the potential development of an adaptive IAP/IAV estimator that rapidly adjusts and corrects for estimation errors arising from possible inter-animal variabilities in perceived cavity compliance during perfusion.

ACKNOWLEDGMENTS

The research in this paper was conducted under IACUC #0121006 at The University of Maryland Medical School, Baltimore, MD (UMB). Support for this research was provided by a National Science Foundation (NSF) Growing Convergence Research (GCR) grant. The authors gratefully acknowledge this support. Any opinions, findings, and conclusions or recommendations expressed in this work are those of the author(s) and not necessarily those of NSF.

REFERENCES

[1] S. R. Carr, J. P. Cantor, A. S. Rao, T. V. Lakshman, J. E. Collins, and J. S. Friedberg, "Peritoneal perfusion with oxygenated perfluorocarbon augments systemic oxygenation," *Chest*, vol. 130, no. 2, pp. 402–411, 2006.

[2] M. Doosthosseini, K. R. Aroom, M. R. Aroom, M. Culligan, W. Naselsky, C. Thamire, H. W. Haslach, S. A. Roller, J. R. Hughen, J. S. Friedberg *et al.*, "Monitoring, control system development, and experimental validation for a novel extrapulmonary respiratory support setup," *IEEE/ASME Transactions on Mechatronics*, 2022.

[3] M. Doosthosseini, Y. Moon, A. Commins, S. Wood, W. Naselsky, M. J. Culligan, K. Aroom, M. Aroom, A. Shah, G. J. Bittle *et al.*, "Estimating the impact of peritoneal perfluorocarbon perfusion on carbon dioxide transport dynamics in a laboratory animal," in *2022 American Control Conference (ACC)*. IEEE, 2022, pp. 3000–3005.

[4] A. Regli, P. Pelosi, and M. L. Malbrain, "Ventilation in patients with intra-abdominal hypertension: what every critical care physician needs to know," *Annals of intensive care*, vol. 9, no. 1, pp. 1–19, 2019.

[5] A. W. Kirkpatrick, D. J. Roberts, J. De Waele, R. Jaeschke, M. L. Malbrain, B. De Keulenaer, J. Duchesne, M. Bjorck, A. Leppaniemi, J. C. Ejike *et al.*, "Intra-abdominal hypertension and the abdominal compartment syndrome: updated consensus definitions and clinical practice guidelines from the world society of the abdominal compartment syndrome," *Intensive care medicine*, vol. 39, no. 7, pp. 1190–1206, 2013.

[6] A. R. Blaser, M. Björck, B. De Keulenaer, and A. Regli, "Abdominal compliance: a bench-to-bedside review," *Journal of Trauma and Acute Care Surgery*, vol. 78, no. 5, pp. 1044–1053, 2015.

[7] M. L. Malbrain, D. Chiumello, P. Pelosi, A. Wilmer, N. Brienza, V. Malcangi, D. Bihari, R. Innes, J. Cohen, P. Singer *et al.*, "Prevalence of intra-abdominal hypertension in critically ill patients: a multicentre epidemiological study," *Intensive care medicine*, vol. 30, no. 5, pp. 822–829, 2004.

[8] A. R. Blaser, A. Regli, B. De Keulenaer, E. J. Kimball, L. Starkopf, W. A. Davis, P. Greiffenstein, J. Starkopf *et al.*, "Incidence, risk factors, and outcomes of intra-abdominal hypertension in critically ill patients—a prospective multicenter study (iroi study)," *Critical care medicine*, vol. 47, no. 4, p. 535, 2019.

[9] R. Scanziani, B. Dozio, I. Baragetti, and S. Maroni, "Intraperitoneal hydrostatic pressure and flow characteristics of peritoneal catheters in automated peritoneal dialysis," *Nephrology Dialysis Transplantation*, vol. 18, no. 11, pp. 2391–2398, 2003.

[10] P. Y. Durand, J. Chanliau, J. Gamberoni, D. Hestin, and M. Kessler, "Apd: clinical measurement of the maximal acceptable intraperitoneal volume," *Advances in peritoneal dialysis*, vol. 10, pp. 63–63, 1994.

[11] A. G. Vilos, G. A. Vilos, B. Abu-Rafea, J. Hollett-Caines, and M. Al-Omran, "Effect of body habitus and parity on the initial veres intraperitoneal co2 insufflation pressure during laparoscopic access in women," *Journal of minimally invasive gynecology*, vol. 13, no. 2, pp. 108–113, 2006.

[12] D. Chiumello, F. Tallarini, M. Chierichetti, F. Polli, G. L. Bassi, G. Motta, S. Azzari, C. Carsenzola, and L. Gattinoni, "The effect of different volumes and temperatures of saline on the bladder pressure measurement in critically ill patients," *Critical care*, vol. 11, no. 4, pp. 1–7, 2007.

[13] O. Yoshino, A. Quail, C. Oldmeadow, and Z. J. Balogh, "The interpretation of intra-abdominal pressures from animal models: the rabbit to human example," *Injury*, vol. 43, no. 2, pp. 169–173, 2012.

[14] T. S. Papavramidis, N. A. Michalopoulos, G. Mistriotis, I. G. Pliakos, I. I. Kesisoglou, and S. T. Papavramidis, "Abdominal compliance, linearity between abdominal pressure and ascitic fluid volume," *Journal of Emergencies, Trauma and Shock*, vol. 4, no. 2, p. 194, 2011.

[15] J. P. Mulier, B. Dillemans, M. Crombach, C. Missant, and A. Sels, "On the abdominal pressure volume relationship," *The Internet Journal of Anesthesiology*, vol. 21, no. 1, pp. 5221–5231, 2009.

[16] M. L. Malbrain, Y. Peeters, and R. Wise, "The neglected role of abdominal compliance in organ-organ interactions," *Critical Care*, vol. 20, no. 1, pp. 1–10, 2016.

[17] A. Regli, B. L. De Keulenaer, B. Singh, L. E. Hockings, B. Noffsinger, and P. V. van Heerden, "The respiratory pressure—abdominal volume curve in a porcine model," *Intensive care medicine experimental*, vol. 5, no. 1, pp. 1–12, 2017.

[18] B. De Keulenaer, J. De Waele, B. Powell, and M. Malbrain, "What is normal intra-abdominal pressure and how is it affected by positioning,

body mass and positive end-expiratory pressure?" *Intensive care medicine*, vol. 35, no. 6, pp. 969–976, 2009.

[19] A. B. Cresswell, W. Jassem, P. Srinivasan, A. A. Prachalias, E. Sizer, W. Burnal, G. Auzinger, P. Muiesan, M. Rela, N. D. Heaton *et al.*, "The effect of body position on compartmental intra-abdominal pressure following liver transplantation," *Annals of intensive care*, vol. 2, no. 1, pp. 1–10, 2012.

[20] M. L. Malbrain, J. J. De Waele, A. W. Kirkpatrick *et al.*, "Intra-abdominal hypertension: definitions, monitoring, interpretation and management," *Best practice & research Clinical anaesthesiology*, vol. 27, no. 2, pp. 249–270, 2013.

[21] R. Chun, L. Baghirzada, C. Tiruta, and A. Kirkpatrick, "Measurement of intra-abdominal pressure in term pregnancy: a pilot study," *International journal of obstetric anesthesia*, vol. 21, no. 2, pp. 135–139, 2012.

[22] J. E. Varela, M. Hinojosa, and N. Nguyen, "Correlations between intra-abdominal pressure and obesity-related co-morbidities," *Surgery for Obesity and Related Diseases*, vol. 5, no. 5, pp. 524–528, 2009.

[23] F. Fuchs, M. Bruyere, M.-V. Senat, E. Purenne, D. Benhamou, and H. Fernandez, "Are standard intra-abdominal pressure values different during pregnancy?" *PLoS One*, vol. 8, no. 10, p. e77324, 2013.

[24] K. Verbeke, I. Casier, B. VanAcker, B. Dillemans, and J. Mulier, "Impact of laparoscopy on the abdominal compliance is determined by the duration of the pneumoperitoneum, the number of gravidity and the existence of a previous laparoscopy or laparotomy: 1ap9–3," *European Journal of Anaesthesiology— EJA*, vol. 27, no. 47, pp. 29–30, 2010.

[25] M. Malbrain, D. J. Roberts, I. De Laet, J. J. De Waele, M. Sugrue, A. Schachtrupp, J. Duchesne, G. Van Ramshorst, B. De Keulenaer, A. W. Kirkpatrick *et al.*, "The role of abdominal compliance, the neglected parameter in critically ill patients-a consensus review of 16. part 1: definitions and pathophysiology," *Anaesthesiology Intensive Therapy*, vol. 46, no. 5, pp. 392–405, 2014.

[26] N. Zaleski, Y. Moon, M. Doosthosseini, G. Hopkins, K. Aroom, M. Aroom, W. Naselsky, M. J. Culligan, J. Leibowitz, A. Shah *et al.*, "Modeling and experimental identification of peritoneal cavity pressure dynamics during oxygenated perfluorocarbon perfusion," in *2022 European Control Conference (ECC)*. IEEE, 2022, pp. 297–302.

[27] P.-Y. Durand, P. Balteau, J. Chanliau, and M. Kessler, "Optimization of fill volumes in automated peritoneal dialysis," *Peritoneal dialysis international*, vol. 20, no. 2_suppl, pp. 83–88, 2000.

[28] Y. Moon, M. Doosthosseini, B. Kadkhodaeielyaderani, J. S. Friedberg, J.-O. Hahn, and H. K. Fathy, "An extended kalman filter for retained volume estimation in peritoneal perfusion applications," in *2022 IEEE Conference on Control Technology and Applications (CCTA)*. IEEE, 2022, pp. 95–101.